Measurement of $^7\mathrm{Li}(n,\gamma_0)^8\mathrm{Li}$ cross sections at $E_n = 1.5$–1340 eV

J. C. Blackmon,[1,2] A. E. Champagne,[2] J. K. Dickens,[1] J. A. Harvey,[1] M. A. Hofstee,[2,*] S. Kopecky,[3] D. C. Larson,[1] D. C. Powell,[2] S. Raman,[1] and M. S. Smith[1]

[1]*Oak Ridge National Laboratory, P.O. Box 2008, Oak Ridge, Tennessee 37831*

[2]*The University of North Carolina at Chapel Hill, Chapel Hill, North Carolina 27599 and Triangle Universities Nuclear Laboratory, Durham, North Carolina 27088*

[3]*Institut für Kernphysik der Technischen Universität Wien, A-1020 Wien, Austria*

(Received 4 January 1996)

The $^7\mathrm{Li}(n,\gamma)^8\mathrm{Li}$ cross section is important in inhomogeneous big bang models, and as a constraint on model parameters used to determine the solar $^7\mathrm{Be}(p,\gamma)^8\mathrm{B}$ reaction rate. Values of the $^7\mathrm{Li}(n,\gamma_0)^8\mathrm{Li}$ reaction cross section were measured for neutron energies between 1.5 and 1340 eV at the Oak Ridge Electron Linear Accelerator. The normalization of the cross section was determined by measuring the gamma-ray yield from the $^7\mathrm{Li}(n,\gamma_0)^8\mathrm{Li}$ reaction relative to that from the $^{10}\mathrm{B}(n,\alpha\gamma)^7\mathrm{Li}$ reaction. The cross section was found to have the inverse neutron-velocity relationship $(1/v)$ indicative of s-wave capture. These results help resolve ambiguities in previous measurements. [S0556-2813(96)04307-5]

PACS number(s): 26.35.+c, 26.65.+t, 25.40.Lw, 28.20.Fc

I. INTRODUCTION

The neutron-capture cross section of $^7\mathrm{Li}$ at low energies is important in nuclear astrophysics for two reasons. First, an inhomogeneous big bang can produce significantly different primordial isotopic abundances than are produced in a standard big bang. In particular, nucleosynthesis in the low-density, neutron-rich regions may produce a greater abundance of CNO nuclei. The $^7\mathrm{Li}(n,\gamma)^8\mathrm{Li}(\alpha,n)^{11}\mathrm{B}(n,\gamma)^{12}\mathrm{B}(\beta^-\nu)^{12}\mathrm{C}$ sequence of reactions bridges the mass gap at $A=8$. The $^7\mathrm{Li}(n,\gamma)^8\mathrm{Li}$ reaction initiates the process, and its rate is crucial in determining the amount of heavier elements produced in an inhomogeneous big bang [1].

Second, the $^7\mathrm{Li}(n,\gamma)^8\mathrm{Li}$ reaction is the mirror reaction to the $^7\mathrm{Be}(p,\gamma)^8\mathrm{B}$ reaction, which is responsible for the production of high-energy solar neutrinos. Most of the neutrinos detected by the Homestake and Kamiokande experiments are produced by this reaction [2–4]. Measurement of the $^7\mathrm{Be}(p,\gamma)^8\mathrm{B}$ reaction at low energies is difficult, and so the cross section at solar energies ($E_p \approx 20$ keV) is determined by an extrapolation from measured cross sections at $E_p > 140$ keV. The extrapolation is performed using a model such as the direct-capture model [5,6] or the microscopic model [7,8]. The $^7\mathrm{Li}(n,\gamma)^8\mathrm{Li}$ reaction is relevant because its cross section constrains the model parameters used in the extrapolation.

Despite several measurements, the $^7\mathrm{Li}(n,\gamma)^8\mathrm{Li}$ cross section is uncertain at neutron energies below 1 MeV. Values of the cross section with a 20% uncertainty were first reported by Imhof *et al.* [9] in the energy range $E_n =$ 40–1000 keV. Cross sections approximately a factor of 2 smaller than those of Imhof *et al.* were reported in the energy range $E_n =$ 25–420 keV by Wiescher, Steininger, and Käppeler [10]. Nagai *et al.* [11] measured the cross section at $E_n = 30$ keV as 39.3 ± 6.0 μb. In a reactor-based measurement, the thermal neutron capture cross section was determined to be 45.4 ± 3.0 mb by Lynn, Jurney, and Raman [12]. Both of these later measurements agree with the original normalization of Imhof *et al.* assuming that the cross section follows the inverse neutron-velocity relationship $(1/v)$ indicative of s-wave capture.

A recent measurement of large analyzing powers in the $^7\mathrm{Li}(\vec{p},\gamma_0)^8\mathrm{Be}$ reaction indicates that there is substantial p-wave capture strength in that reaction at low energies [13]. The mechanism responsible for this anomalous result is not known [14]. If the physical origin lies in a direct mechanism, it would impact other low-energy capture reactions on light-mass isotopes. In particular, there could be p-wave capture strength in the $^7\mathrm{Li}(n,\gamma)^8\mathrm{Li}$ reaction, which has the same target nucleus.

We have measured absolute $^7\mathrm{Li}(n,\gamma_0)^8\mathrm{Li}$ cross sections for neutron energies in the range 1.5–1340 eV. The experimental procedure is discussed in the following section, and the results are presented in Sec. III. The implications of these results are discussed in Sec. IV.

II. EXPERIMENTAL PROCEDURE

This experiment was conducted at the Oak Ridge Electron Linear Accelerator (ORELA) [15,16]. A pulsed 140-MeV electron beam is stopped in a water-cooled tantalum target, and the resulting bremsstrahlung acts as a white source of neutrons. The neutrons travel down evacuated flight tubes to experimental stations and their energies are determined by measuring their time of flight. A schematic representation of the experimental setup is shown in Fig. 1. This experiment was conducted at the 20-m station, with a neutron flight path of 18.89 m. The electron beam was pulsed at rates of 400 and 530 Hz with pulse widths from 8 to 30 ns. Neutrons with energies less than 0.4 eV were absorbed from the beam with

[*]Present address: Colorado School of Mines, Golden, CO 80401-1887.

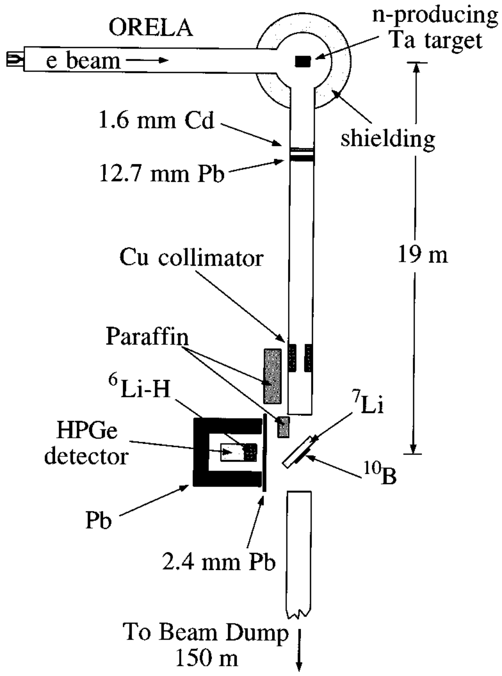

FIG. 1. Schematic diagram of the experimental setup.

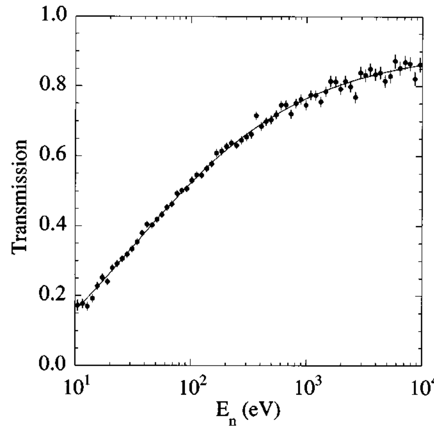

FIG. 2. Neutron transmission through 0.277 g/cm^2 of the boron powder. The solid curve is the result of a fit to the data assuming the functional form given in Eq. (2).

a 1.6-mm-thick piece of cadmium. The size of the neutron beam was defined by a 0.6-m-long copper collimator. The collimator is cylindrical in shape, but slightly tapered with an inside diameter between 8.1 and 8.3 cm.

The ^{7}Li sample was manufactured at Oak Ridge National Laboratory and consisted of 78.77 g of 99.993%-enriched ^{7}Li. The lithium was sealed between two thin pieces of stainless steel and covered an area of 232 cm^2. The target thickness was specified to be uniform to better than 5%, giving an areal target density of 0.340$\pm$0.017 g/cm^2. The capture gamma rays from the $^7\mathrm{Li}(n,\gamma_0)^8\mathrm{Li}$ reaction were detected with a 132-cm^3 high-purity n-type germanium detector. The detector was placed 30 cm from the center of the target at θ=90°. The 2033-keV gamma ray from capture to the ground state in ^{8}Li was observed in this measurement. Capture also proceeds in a cascade through the first-excited state at E_x=981 keV, producing gamma rays with energies of 981 and 1052 keV with equal intensity. However, this branch was too weak to be observed (branching ratio of 0.106$\pm$0.010 with thermal neutrons [12]).

To determine the overall normalization of the cross section, it was necessary to determine the neutron flux, detector efficiency, and number of sample atoms. We affixed a thin ^{10}B sample to the downstream side of the ^{7}Li sample and determined the neutron flux by concurrently measuring the yield of the 478-keV gamma ray arising from the $^{10}\mathrm{B}(n,\alpha\gamma)^7\mathrm{Li}$ reaction along with the $^7\mathrm{Li}(n,\gamma_0)^8\mathrm{Li}$ gamma ray of interest. The cross section for the ^{10}B reaction is known to high accuracy. Because of its large magnitude and $1/v$ neutron energy dependence, it is commonly used as a calibration standard in neutron experiments [17,18]. The cross section for the $^7\mathrm{Li}(n,\gamma_0)^8\mathrm{Li}$ reaction, σ_{Li}, is then related to the cross section for the $^{10}\mathrm{B}(n,\alpha\gamma)^7\mathrm{Li}$ reaction, σ_{B}, by

$$\sigma_{\mathrm{Li}}=\frac{C_{\mathrm{Li}}}{C_{\mathrm{B}}}\frac{\varepsilon_{\mathrm{B}}}{\varepsilon_{\mathrm{Li}}}\frac{N_{\mathrm{B}}}{N_{\mathrm{Li}}}\sigma_{\mathrm{B}}, \tag{1}$$

where C_{B} is the number of gamma rays observed from the $^{10}\mathrm{B}(n,\alpha\gamma)^7\mathrm{Li}$ reaction and C_{Li} is the number of counts observed from the $^7\mathrm{Li}(n,\gamma_0)^8\mathrm{Li}$ reaction. The total number of ^{10}B and ^{7}Li target atoms is denoted by N_{B} and N_{Li}, and ε_{B} and $\varepsilon_{\mathrm{Li}}$ are the photopeak efficiencies of the detector at 478 keV and 2033 keV, respectively.

The thin ^{10}B sample was produced by dispersing 0.39$\pm$0.03 g of an enriched powder over an area of 46 cm^2 between two pieces of adhesive tape. The powder was specified to be 92% enriched, and its chemical composition was believed to be B_4C. A neutron transmission measurement was performed at ORELA to determine the mass fraction of ^{10}B in the powder, and hence determine the number of ^{10}B target atoms. A thick sample (0.277 g/cm^2) was prepared from the same powder, and the transmission through the thick sample was measured with a ^{6}Li-glass scintillation detector for neutron energies of E_n= 1–10^5 eV. The ^{10}B content was determined by fitting the transmission T with a function of the form

$$T=e^{-p_1}e^{-p_2/\sqrt{E}}, \tag{2}$$

where p_i are the fit parameters. The first exponential is an energy-independent term, and the second accounts for the $1/v$ cross section of the $^{10}\mathrm{B}(n,\alpha)^7\mathrm{Li}$ reaction. The results are shown in Fig. 2 along with the fit to the data. The amount of ^{10}B in the thick sample was found to be $0.150\pm0.003_{\mathrm{stat}}\pm0.003_{\mathrm{sys}}$ g/cm^2. Therefore, the powder is 54% ^{10}B by mass. The remaining fraction of the mass of the sample is ^{11}B, carbon, and water. This was confirmed in a separate experiment, performed at the University of North Carolina at Chapel Hill, by pressing a sample of the powder and measuring the scattering yield of 2-MeV alpha particles observed at 165°. The total number of ^{10}B atoms in the thin sample used in the $^7\mathrm{Li}(n,\gamma)^8\mathrm{Li}$ measurement is 0.0211$\pm$0.0017 mol, where the uncertainty results from adding the uncertainty in the mass of the sample and the uncertainties from the transmission measurement in quadrature.

The boron sample was smaller in size than the neutron beam, and so the ratio of target atoms depends upon the beam profile. The size and location of the beam were measured at the sample position with photographic film. The film shows a uniformly irradiated area with a 8.7-cm diameter, consistent with the projection from the tantalum target through the copper beam collimator and onto the sample. The film also shows a beam halo extending to a diameter of 9.3 cm. Since the film is exposed by electromagnetic radiation, it does not necessarily provide an accurate representation of the intensity of the neutron flux. However, previous experiments which mapped the neutron flux from ORELA using a small scintillator detector found the flux to be consistent with photographic measurements. These flux mappings also showed the neutron flux to be uniform over the central (90–95)% of the beam spot. To test the uniformity of the neutron flux in this experiment, we measured the yield from a 1-cm-diam ^{10}B test sample as a function of sample position. After correcting for the change in detector efficiency with position, the counting rate was found to be constant within the 5% counting statistics over the central 8.7-cm diameter of the beam. The counting rate decreased in the halo, but the size of the test sample was too large to accurately map the intensity of the flux in the halo.

We take the neutron flux to be uniform in position. The number of ^7Li target atoms is determined by scaling the total mass of the sample by the ratio of the beam size on target to the total area of the sample. We take the beam diameter to include half the halo, and adopt an uncertainty on the resulting area such that $\pm 2\sigma$ covers the entire halo area of the beam. The sample was oriented at 45° with respect to the beam axis, and the illuminated area of the target was (91 ± 3) cm^2. This gives the number of ^7Li target atoms to be (4.4 ± 0.3) mol, where the uncertainty in the number of atoms results from adding the uncertainty in the size of the neutron beam in quadrature with the possible 5% variation in the thickness.

Because of the small cross section for the $^7Li(n,\gamma_0)\,^8Li$ reaction, particular attention was given to reducing background. To attenuate the flux of neutrons and gamma rays scattered from beam collimators and other external sources, the detector was surrounded by an approximately 10-cm-thick layer of lead and by paraffin blocks. A 100-cm^2 opening was left where the detector faced the sample. With this shielding in place, the primary sources of background were neutrons and low-energy gamma rays scattered by the sample. The gamma-ray background was reduced by placing a 12.7-mm-thick lead filter directly in the beam and by putting a 2.4-mm-thick lead sheet in front of the detector. The background induced by scattered neutrons from the sample was minimized by placing an 8-cm-thick layer of ^6LiH in front of the detector as a neutron absorber. Although the ^6LiH was found to significantly reduce the neutron flux into the detector, scattered neutrons were still the dominant source of background in this experiment.

The efficiency of the detector system was determined *in situ* by measuring the yield from nine calibrated sources (^{60}Co, ^{85}Kr, ^{94}Nb, ^{133}Ba, ^{137}Cs, ^{152}Eu, ^{207}Bi, ^{226}Ra, and ^{249}Cf) placed at the sample location. These sources provided a measurement of the detector efficiency at 43 different energies between 242 keV and 2448 keV. The efficiency of the detector at the energies of interest was determined by interpolation. The photopeak efficiency of the detector was found to be $(1.82\pm0.02)\times10^{-4}$ at 478 keV and $(8.86\pm0.01)\times10^{-5}$ at 2033 keV.

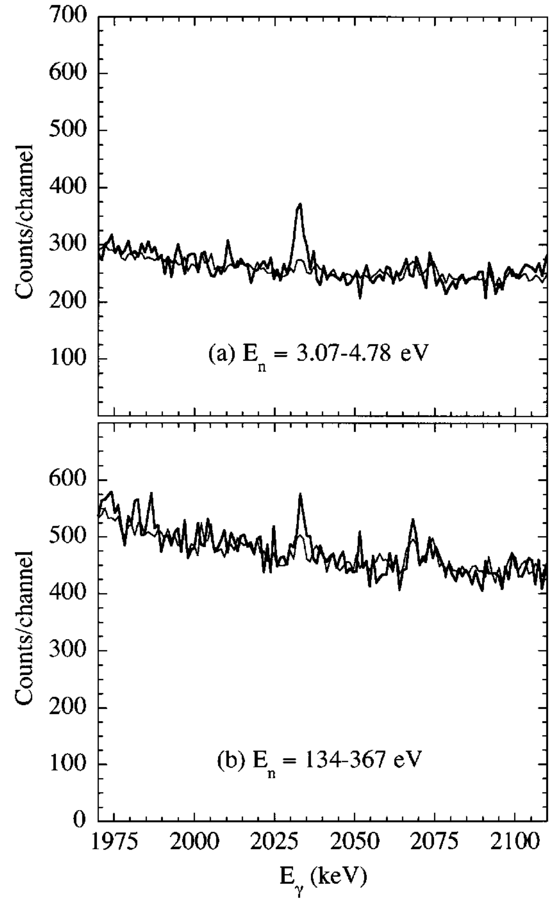

FIG. 3. Gamma-ray energy spectrum showing the region around $E_\gamma = 2033$ keV. The heavy line is the raw spectrum taken with the ^7Li target. The light line is the background data collected with the scattering sample, which have been normalized to the ^7Li data outside the region of the 2033-keV peak.

III. RESULTS

A total of 266 h of data was collected at an average ORELA beam power of about 6 kW. Events were sorted into neutron energy bins in software using the neutron time of flight converted with an EG&G TD 100 time digitizer. Data were stored for neutron energies from 1.5 eV to 1.0 MeV. The 2033-keV peak from the $^7Li(n,\gamma_0)\,^8Li$ reaction was observed in the ten lowest neutron energy bins, which ranged from 1.5 eV to 1340 eV. The energy region of the gamma-ray spectrum around 2033 keV is shown for two of these ten spectra in Fig. 3.

As mentioned previously, the background arises primarily from neutrons scattered by the sample and interacting with the detector. This source presents added difficulty because the $^{70}Ge(n,\gamma)\,^{71}Ge$ reaction also gives rise to a 2033-keV gamma ray [19,20] which contributes to the peak of interest. To estimate this contribution, we collected background data using a sample which was constructed to model neutron scattering from the ^7Li sample. This scattering sample consisted of 30 g of ^9Be together with two thin pieces of stainless steel and the thin boron target. The ^{9}Be isotope was chosen because it has a negligible cross section for the production of gamma rays and a neutron scattering cross section comparable to that of ^{7}Li. Spectra collected with this scattering sample exhibited the same shape for neutron energies between 1 eV and 1340 eV, and so the counts were integrated over this wide neutron energy range to give better statistics. The resulting spectrum was used as a background spectrum for the $^7\mathrm{Li}(n,\gamma_0)^8\mathrm{Li}$ measurement.

The number of counts from the $^7\mathrm{Li}(n,\gamma_0)^8\mathrm{Li}$ reaction was determined by two methods. First, the background spectrum was normalized to each of the spectra taken with the ^{7}Li sample by fitting featureless regions. Normalized background spectra are also shown in Fig. 3. The normalized background spectrum was then subtracted from the corresponding ^{7}Li spectrum, and the remaining counts in the region of the 2033-keV peak were integrated. Second, the ^{7}Li spectra were fit with the background spectrum plus a Gaussian. The MINUIT parameter optimization package [21] was used to perform a χ^2 minimization with a four-parameter function of the form

$$C_{\mathrm{Li}}(E_\gamma)=p_1C_{\mathrm{scat}}(E_\gamma)+p_2\exp\left(-\frac{(E_\gamma-2033\ \mathrm{keV}-p_3)^2}{2p_4{}^2}\right), \tag{3}$$

where p_i are the fitting parameters, and $C_{\mathrm{scat}}(E_\gamma)$ is the spectrum taken with the neutron scattering sample. The number of counts and uncertainties were determined from the best-fit parameter values. Correlations among the parameters were accounted for in computing the uncertainties by using the covariance matrix estimates supplied by MINUIT. The value of the reduced χ^2, χ^2_ν, depends upon the region of the spectrum that is fit, but all reasonable fitting regions were found to converge to the same set of parameters with χ^2_ν values typically in the 1.1–1.3 range. The number of counts determined from the fits agreed within one standard deviation with the number of counts determined from the straight subtraction. The uncertainty in the number of counts from the MINUIT covariance matrix was typically (10–20)% higher than obtained by taking the square root of the number of counts in the region of the peak. We adopt both the number of counts and the more conservative uncertainties from the MINUIT fits.

There were more than 2×10^5 counts from the $^{10}\mathrm{B}(n,\alpha\gamma)^7\mathrm{Li}$ reaction in each of the ^{7}Li spectra, and so determination of the number of counts in this peak was straightforward. The $^{10}\mathrm{B}(n,\alpha\gamma)^7\mathrm{Li}$ cross section for each energy bin was calculated from the ENDF/B-VI evaluated cross section [17] using the average energy of the bin. The average energy E_{ave} was determined from

$$E_{\mathrm{ave}}=\frac{\int En(E)\sigma(E)dE}{\int n(E)\sigma(E)dE}, \tag{4}$$

where the cross section σ was assumed to have a $1/v$ energy dependence and the ORELA neutron flux n is

$$n(E)=AE^{-0.8}, \tag{5}$$

TABLE I. Measured values of the $^7\mathrm{Li}(n,\gamma_0)^8\mathrm{Li}$ cross section.

E_n range (eV)	E_{ave} (eV)	σ_{Li} (mb)
1.48–2.14	1.78	4.2 ± 0.6
2.14–3.07	2.56	3.0 ± 0.6
3.07–4.78	3.84	3.0 ± 0.4
4.78–7.20	5.88	2.0 ± 0.4
7.20–11.5	9.14	2.4 ± 0.4
11.5–23.1	16.4	1.4 ± 0.2
23.1–48.7	33.9	0.94 ± 0.16
48.7–134	82.2	0.74 ± 0.12
134–367	226	0.31 ± 0.09
367–1340	721	0.21 ± 0.06
1340–2870	1980	<0.26

where A is a constant [22]. As a check, the neutron flux was calculated from the gamma-ray yield of the $^{10}\mathrm{B}(n,\alpha\gamma)^7\mathrm{Li}$ reaction and found to be consistent with that assumed in Eq. (5).

The number of gamma rays observed, detector efficiencies, and number of target atoms were combined with the $^{10}\mathrm{B}(n,\alpha\gamma)^7\mathrm{Li}$ cross section to give the $^7\mathrm{Li}(n,\gamma_0)^8\mathrm{Li}$ cross section using Eq. (1). The results are given in Table I. The range of the neutron energy bins and the weighted average energy for each bin are also given. The 2033-keV peak was not observed for $E_n>1340$ keV, but we also include an upper limit for the 11th bin, which ranges in energy from 1340 to 2870 eV.

A correction has been made to account for the attenuation of the neutron flux in the samples. The largest attenuation is caused by neutron capture in the ^{10}B sample. This reduces the number of counts observed from the $^{10}\mathrm{B}(n,\alpha\gamma)^7\mathrm{Li}$ reaction in the $E_n=1.78$ eV spectrum by 9% over that expected if there was no flux attenuation. The correction reduces with increasing neutron energy due to the $1/v$ energy dependence of the cross section. There is also a small correction required due to neutron scattering in the ^{7}Li sample. This correction is about 2% and is constant with neutron energy. There is no significant attenuation ($<1\%$) in either of the sample holders, the stainless steel holding the ^{7}Li, or the tape holding the boron. The total correction made to the data ranges from 11% for the lowest neutron-energy bin to 2% for the highest neutron-energy bin.

IV. CONCLUSIONS

We have measured the $^7\mathrm{Li}(n,\gamma_0)^8\mathrm{Li}$ cross section at energies in the 1.5–1340 eV range. Capture by emission of a 1052-keV gamma ray to the first-excited state in ^{8}Li was not observed. This is expected given the sensitivity of this measurement and the small branching ratio. If we take the branching to the first-excited state to be the same as at thermal energies, then the total neutron-capture cross section is given by dividing the ground-state capture cross section by the 0.894 branching ratio [12]. Our results were scaled by this factor, and they are plotted in Fig. 4 along with the results of previous measurements. Also shown in Fig. 4 is a

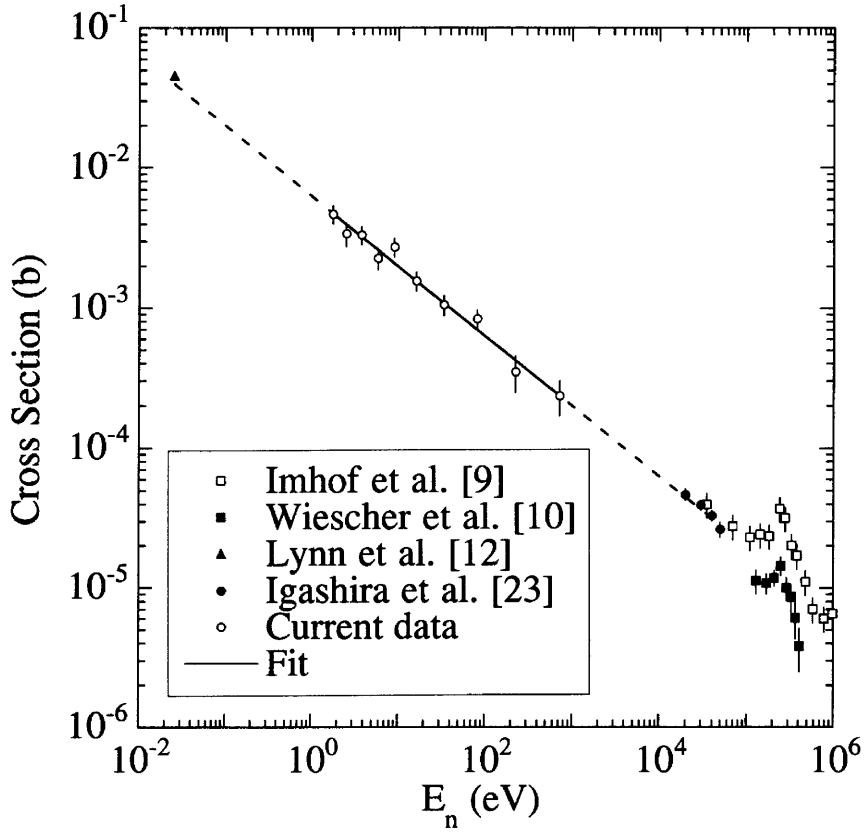

FIG. 4. Measurements of cross sections for the ^{7}Li$(n,\gamma)^8$Li capture reaction. The solid line is a $1/v$ fit to the data from the current measurement.

parametrization of the present data using the form

$$\sigma_{\mathrm{Li}}=\frac{a}{\sqrt{E}}. \tag{6}$$

No deviation from $1/v$ s-wave capture is observed, and the best-fit value of a is $(6.3\pm0.3)\times10^{-3}$ b (eV)$^{1/2}$. The data were also fit by adding additional terms, such as an energy-independent term, but the best-fit values for each of these terms were consistent with zero.

The uncertainties shown in the figure are statistical only. The primary source of systematic uncertainty in this measurement is the ratio of ^{7}Li to ^{10}B target atoms. The uncertainty in the number of ^{7}Li target atoms is 7%, while the uncertainty in the number of ^{10}B atoms is 8%. Uncertainties from the detector efficiency and ^{10}B cross section are 1%. Thus, we estimate the systematic uncertainty in this measurement to be 11%.

Extrapolating the fit to our data gives a thermal cross section of $40\pm2_{\mathrm{stat}}\pm4_{\mathrm{sys}}$ mb. This is consistent with the directly measured value of 45.4 ± 3.0 mb [12]. The extrapolation of our fit to higher energies is in agreement with the results of the original measurement of Imhof *et al.* [9] and with the results of a recent measurement by Igashira *et al.* [23] at neutron energies between 20 and 50 keV. The results of these recent measurements support using the larger value of the ^{7}Li$(n,\gamma)^8$Li reaction rate quoted by Malaney and Fowler [24] (based upon the measurement of Imhof *et al.*) rather than the smaller rate of Wiescher, Steininger, and Käppeler [10].

With approximately 1 month of additional running, we could extend this measurement up to $E_n\approx10$ keV. However, such an effort does not appear warranted. Given the results of this measurement and that of Igashira *et al.* [23], it seems unlikely that the ^{7}Li$(n,\gamma)^8$Li cross section exhibits an energy dependence significantly different from $1/v$. The mechanism which results in the large p-wave component seen in proton capture on ^{7}Li must not play a significant role in neutron capture on the same nucleus. This fact could be evidence that the p-wave capture arises from an isospin-dependent compound-nucleus interaction. However, it is also possible that the p-wave strength could be the result of a direct reaction mechanism which is suppressed in neutron capture on ^{7}Li. This might occur if the p-wave capture is associated with the ^{7}Li wave function at large radii, because neutrons are more sensitive to the interior portion of the wave function. Clearly, more theoretical work is needed to determine the origin of this interesting effect.

ACKNOWLEDGMENTS

The authors would like to thank N. Parikh for performing the alpha-particle scattering experiment on the ^{10}B sample. This work supported in part by the U.S. Department of Energy under Contract No. DE-FG05-88ER40442. Oak Ridge National Laboratory is managed by Lockheed Martin Energy Research Corp. for the U.S. Department of Energy under Contract No. DE-AC05-96OR22464.

[1] L. H. Kawano, W. A. Fowler, R. W. Kavanagh, and R. A. Malaney, Astrophys. J. **372**, 1 (1991).

[2] B. T. Cleveland, T. Daily, R. Davies, J. Distel, K. Lande, C. K. Lee, P. Wildenhain, and J. Ullman, Nucl. Phys. **B38**, 47 (1995).

[3] Y. Suzuki, Nucl. Phys. **B38**, 54 (1995).

[4] J. N. Bahcall and R. K. Ulrich, Rev. Mod. Phys. **60**, 297 (1988).

[5] B. W. Filippone, A. J. Elwyn, C. N. Davids, and D. D. Koetke, Phys. Rev. C **28**, 2222 (1983).

[6] T. A. Tombrello, Nucl. Phys. **71**, 459 (1965).

[7] P. Descouvemont and D. Baye, Nucl. Phys. **A567**, 341 (1994).

[8] P. Descouvemont and D. Baye, Nucl. Phys. **A487**, 420 (1988).

[9] W. L. Imhof, R. G. Johnson, F. J. Vaughn, and M. Walt, Phys. Rev. **114**, 1037 (1959).

[10] M. Wiescher, R. Steininger, and F. Käppeler, Astrophys. J. **344**, 464 (1989).

[11] Y. Nagai, M. Igashira, N. Mukai, T. Ohsaki, F. Uesawa, K. Takeda, T. Ando, H. Kitzawa, S. Kubono, and T. Fukuda, Astrophys. J. **381**, 444 (1991).

[12] J. E. Lynn, E. T. Jurney, and S. Raman, Phys. Rev. C **44**, 764 (1991).

[13] R. M. Chasteler, H. R. Weller, D. R. Tilley, and R. M. Prior, Phys. Rev. Lett. **72**, 3949 (1994).

[14] H. R. Weller and R. M. Chasteler, Z. Phys. A **352**, 353 (1995).

[15] R. A. Schrack, O. A. Wasson, D. C. Larson, J. K. Dickens, and J. H. Todd, Nucl. Sci. Eng. **114**, 352 (1993).

[16] D. C. Larson and J. K. Dickens, Phys. Rev. C **39**, 1736 (1989).

[17] A. D. Carlson, W. P. Poenitz, G. M. Hale, and R. W. Peelle, in *Nuclear Data for Basic and Applied Science*, edited by P. G. Young, R. E. Brown, G. F. Auchampaugh, P. W. Lisowski, and L. Stewart (Gordon and Breach, New York, 1986), p. 1429.

[18] R. G. Downing, G. P. Lamaze, J. K. Langland, and S. T. Hwang, J. Res. Natl. Inst. Stand. Technol. **98**, 109 (1993).

[19] C. Hofmeyr, B. C. Winkler, J. A. M. DeVilliers, J. G. Malan, and J. W. Tepel, in *Neutron Capture Gamma-Ray Spectroscopy*, edited by N. Ryde (International Atomic Energy Agency, Vienna, 1969), p. 301.

[20] M. R. Bhat and D. E. Alburger, Nucl. Data Sheets **53**, 1 (1988).

[21] F. James and M. Roos, Comput. Phys. Commun. **10**, 343 (1975).

[22] S. N. Cramer and F. G. Perey, Nucl. Sci. Eng. **111**, 102 (1992).

[23] M. Igashira *et al.* (private communication).

[24] R. A. Malaney and W. A. Fowler, in *The Origin and Distribution of the Elements*, edited by G. J. Mathews (World Scientific, Singapore, 1987), p. 76.